Journal of Neuropathology and Experimental Neurology

Vol. 56, No. 10
October, 1997
pp. 1132–1141

Temporal and Regional Patterns of Axonal Damage following Traumatic Brain Injury: A Beta-amyloid Precursor Protein Immunocytochemical Study in Rats

HELEN M. BRAMLETT, MS, SUSAN KRAYDIEH, BS, EDWARD J. GREEN, PHD, W. DALTON DIETRICH, PHD

Abstract. Diffuse axonal injury (DAI) is an important consequence of human head trauma. This experimental investigation utilized the immunocytochemical visualization of beta-amyloid precursor protein (beta-APP) to document regional patterns of axonal injury after traumatic brain injury (TBI) and to determine the importance of injury severity on the magnitude of axonal damage. Rats underwent moderate (1.84–2.11 atm) or severe (2.38–2.52 atm) parasagittal fluid-percussion (F-P) brain injury or sham procedures. At 1, 3, 7 or 30 days after TBI, rats were perfusion-fixed and sections immunostained for the visualization of beta-APP. A regionally specific axonal response to TBI was documented after moderate F-P injury. Within the dorsolateral striatum, an early increase in beta-APP-positive axonal profiles at 24 hours (h) was followed by a significant decline at subsequent survival periods. In contrast, the frequency of reactive profiles was initially low within the thalamus, but increased significantly by day 7. Within the external capsule at the injury epicenter, numbers of immunoreactive axons increased significantly at 24 h and remained elevated throughout the subsequent survival periods. At multiple periods after TBI, selective cortical and thalamic neurons displayed increased staining of the perikarya. A significant increase in the overall frequency of beta-APP profiles was documented in the severe vs moderately injured rats at 72 h after TBI. These data indicate that parasagittal F-P brain injury (a) results in widespread axonal damage, (b) that axonal damage includes both reversible and delayed patterns, and (c) that injury severity is an important factor in determining the severity of the axonal response to TBI.

Key Words: Beta-amyloid precursor protein; Diffuse axonal injury; Fluid-percussion; Head injury; Immunocytochemistry.

INTRODUCTION

Diffuse axonal injury (DAI) is the most common cause of vegetative state and severe disability in nonmissile head injury (1). Diffuse axonal injury not accompanied by an intracranial mass lesion occurs in almost 50% of patients with a severe head injury and causes 35% of all deaths (2). This type of brain damage was initially termed "diffuse degeneration of white matter" and has been characterized by a variety of other descriptive terms (3). According to Adams (4), severe DAI can be classified into 3 distinctive features: (a) focal lesions of the corpus callosum; (b) focal lesions of various sizes within the rostral midbrain; and (c) microscopic evidence of widespread damage to axons. Incidences of DAI due to mild head trauma can be seen without any apparent macroscopic changes in the brain. The presence of axonal retraction balls visualized by classical silver staining methods has been extensively used to demonstrate the time course of these axonal changes. Using this methodology, the visualization of argyrophilic axonal retraction balls has generally been reported to take 16–72 h to become fully developed after human traumatic brain injury (5).

Recently, ultrastructural and immunocytochemical investigations have provided evidence for reactive axonal changes occurring much earlier after TBI (6–16). For example, Grady and colleagues (6) reported reactive axonal changes at 6 h postinjury with antibodies targeted at the 68 kD neurofilament subunit. More recently, the immunocytochemical visualization of beta-amyloid precursor protein (beta-APP) has been found to be a useful marker for axonal damage in clinical studies (9–13). For example, Sherrif et al (12) reported axonal beta-APP immunoreactivity in cases that had survived 3 h or more. McKenzie and colleagues (13) directly compared conventional silver impregnation techniques with beta-APP immunohistochemistry and reported that the latter technique was more sensitive for identifying axonal injury. In that study, axonal damage after only 2 h of survival was demonstrated and damage was shown to progress with increased survival periods. The accumulation of beta-APP at sites of axonal injury results from disruption of the cytoskeleton, leading to abnormalities in the axonal transport of beta-APP (13).

Several experimental studies have also used beta-APP as a marker of axonal damage (14–16). Otsuka and colleagues (14) first reported increased beta-APP immunoreactivity in damaged axons following a needle stab injury. With focal compression contusion trauma, Lewen et al (15) observed immunoreactive axons within subcortical white matter and thalamus 21 days after injury. Pierce and colleagues (16), in a model of lateral fluid-percussion (F-P) brain injury, examined alterations in the distribution of amyloid precursor proteins/amyloid precursor protein-like proteins (APP/APLP) at several time periods after moderate to severe injury. Numerous APP/APLP-positive axonal swellings were reported in the thalamus as early as 1 h and in other areas within 2 h after injury.

From the Neurotrauma Research Center, Departments of Neurology and Psychology, University of Miami School of Medicine, Miami, FL, 33101.

Correspondence to: W. Dalton Dietrich, PhD, Department of Neurology (D4-5), University of Miami School of Medicine, P.O. Box 016960, Miami, FL 33101.

This study was supported in part by NIH Grant NS30291. We thank Helen Valkowitz for helping in the preparation of the manuscript.

Over the last several years, our laboratory has documented the acute and more chronic histopathological consequences of moderate parasagittal F-P brain injury (17–20). At 1 h after TBI, a gliding hemorrhagic contusion overlying the lateral external capsule was documented (17). At 3 days, necrotic neurons were seen within the CA3 hippocampus, dentate hilus, lateral parietal cortex and lateral thalamus of the traumatized hemisphere (18, 19). Light and electron microscopic studies have also demonstrated widespread axonal damage 24 h after TBI (19). At 2 months after TBI, enlargement of the ipsilateral lateral ventricle was associated with atrophy of ipsilateral gray matter structures (20). In clinical investigations of chronically brain injured patients, ventricular enlargement has been hypothesized to result from atrophy of both gray matter and white matter tracks (21–24).

Although axonal injury plays a major role in the morbidity and mortality associated with TBI, few experimental studies have evaluated the temporal and regional patterns of axonal injury in an experimental TBI model. The major purpose of this study was to quantitate regional patterns of axonal damage using beta-APP immunocytochemistry at several time periods after TBI. In addition, we sought to determine whether evidence for reversible axonal damage could be demonstrated. Finally, the effects of injury severity on this important outcome measure was assessed.

MATERIALS AND METHODS

Traumatic Brain Injury

Thirty male Sprague-Dawley rats, weighing between 265 and 410 g, were used for this experiment. Animals were maintained on a 12/12 (light/dark) cycle and given food ad libitum. The principles of laboratory animal care (NIH publication No. 86-23, revised 1985) were followed for these experiments. Animals were anesthetized 24 h prior to injury with equitensin (1.0 ml) and were surgically prepared for fluid-percussion (F-P) injury as described previously (17, 20). Briefly, a parasagittal craniotomy (4.8 mm) was performed at 3.9 mm posterior to bregma and 2.5 mm lateral to the midline (25). A plastic injury tube was next placed over the exposed dura and bonded by adhesive. Dental acrylic was used to affix the injury tube to the skull. The scalp was then sutured closed and the animal was allowed to recover before being returned to the home cage.

After fasting overnight, an F-P device was used to produce experimental TBI via the injury tube (26, 27). Intubated anesthetized rats (70% nitrous oxide, 0.5% halothane, and 30% oxygen) were subjected to a moderate (1.82–2.11 atm) or severe (2.38–2.52 atm) pressure pulse. Prior to TBI, a catheter was placed in the right femoral artery to monitor arterial blood pressure and blood gases. Brain temperature was indirectly measured by a thermistor placed in the left temporalis muscle and maintained at a normothermic (37°C) level prior and subsequent to TBI. Rectal temperature was also maintained at normothermic levels. Sham animals underwent all surgical procedures but were not subjected to the F-P pulse. Moderately injured animals were sacrificed at 24 h (TBI-24 h, n = 6; sham-24 h, n = 3), 72 h (TBI-72 h; n = 6; sham-72 h, n = 3), 7 days (TBI-7 days; n = 6; sham-7 days, n = 3), and 30 days (TBI-30 days; n = 6; sham-30 days, n = 3). Animals undergoing severe F-P injury were sacrificed at 72 h (TBI-severe, n = 6).

Beta-APP Immunohistochemistry

At various periods after F-P injury, animals were anesthetized and perfused transcardially with isotonic saline at a pressure of 100–120 mm Hg for 15 seconds. This was followed by fixative for 20 minutes (min)(FAM, a mixture of 40% formaldehyde, glacial acetic acid and absolute ethanol; 1:1:8 by volume). Following the perfusions, the heads were immersed in FAM at 4°C for 24 h. The brains were then blocked and embedded in paraffin for tissue sectioning. Two consecutive tissue sections (10 μm thickness) were taken at 300 μm intervals. Sections were mounted on slides and placed in an oven overnight. Slides were rehydrated and placed in 6% H_2O_2 to block endogenous peroxidase activity. The tissue was rinsed and placed in a solution of citrate buffer and microwaved for 15 min. Sections were dipped in 0.05M PBS and incubated with normal horse serum. Primary antibody (Boehringer Mannheim, clone 22C11) (dilution 1:500) was applied and slides were placed in the refrigerator overnight. To test for nonspecific staining, negative controls were conducted where the primary antibody was omitted during tissue processing. Further rinsing was done with PBS and secondary antibody applied. Avidin-Biotin (Vector, Burlingham, CA) complex was used for antibody detection along with DAB to increase staining intensity. Slides were washed in 0.5% Triton X-100, followed by 1% cupric sulfate to further intensify staining. Counterstaining was done with hematoxylin and tissue was then dehydrated and coverslipped. Other serial cut sections were stained for hematoxylin and eosin for routine histopathological assessment.

Beta-APP Regional Quantitation

Beta-APP profiles were identified by their dark brown appearance and elongated or circular shape. These reactive profiles appeared to be retraction balls/bulbs or reactive axonal processes. Profiles were counted per high microscopic field at 400× for the following structures at various coronal levels according to Paxinos and Watson (25): dorsolateral striatum (DLS) (0.8 posterior to bregma), internal capsule (IC), subthalamic radiation (STR), and cerebral cortex (CTX) (3.8 posterior to bregma). Counts were also performed in the external capsule (EC) at 3 coronal levels (0.8, 3.8 and 6.3 posterior to bregma). Averages were computed for each animal from 2 serial sections per coronal level per structure.

Statistical Analysis

The number of beta-APP profiles are expressed as mean values ± standard error (SEM). The external capsule data were analyzed using two-way ANOVA with coronal level as the within-subject factor and the time point when the animal was sacrificed as the between-subjects factor. Data from the other structures were analyzed using one-way ANOVA. Post-hoc mean comparisons were accomplished using Fisher's procedure.

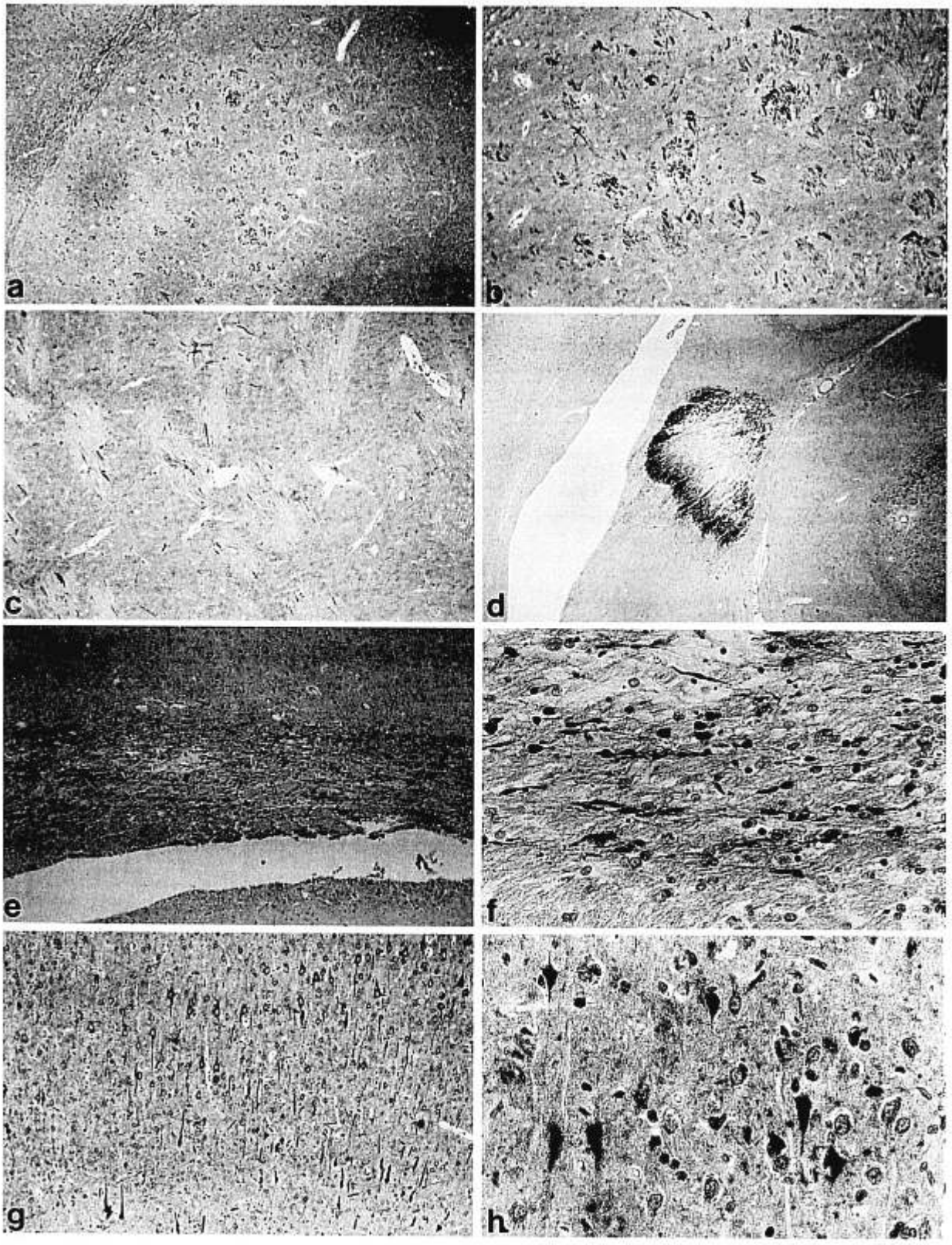

Fig. 1. Beta-amyloid precusor protein (beta-APP) immunoreactivity after moderate TBI. (A) Immunoreactive axonal profiles within dorsolateral striatum 24 h after TBI (×110). (B) Higher magnification of immunoreactive profiles within white matter fascicles of striatum (×280). (C) At 72 h after TBI, fewer reactive profiles are observed within striatum (×280). (D) Dense cluster of reactive profiles within fimbria of hippocampus consistent with primary axotomy (axonal shearing) (×280). (E) Large numbers of immunoreactive profiles within lateral external capsule 24 h after TBI (×280). (F) High magnification of reactive

RESULTS

Patterns of Beta-APP Immunoreactivity

In sham-operated control rats, immunoreactivity was absent within white matter tracts and selective neuronal perikarya were faintly stained with beta-APP. At 24 h after moderate TBI, widespread immunoreactive axonal profiles were observed throughout the traumatized hemispheres (Figs. 1, 2). Numerous reactive profiles were detected within the ipsilateral striatum 24 h after TBI (Fig. 1a, b). Reactive profiles were observed within white matter fascicles coursing through the striatum (Fig. 1b). A dramatic decrease in the frequency of axonal profiles was seen within the striatum at 3 days compared with 24 h (Fig. 1c). Within the hippocampus, reactive profiles were visualized within the alveus and fimbra. In some animals, a focal area of beta-APP accumulation was also seen within the fimbra. This severe axonal response appeared to be due to primary axotomy (Fig. 1d).

Within the external capsule, reactive profiles were numerous and appeared as round or oval profiles of beta-APP (Fig. 1e, f). Reactive profiles were observed within the external capsule of coronal sections spanning levels 1.7 mm anterior to bregma to 7.8 mm posterior to bregma. Reactive axonal profiles were also observed within the cingulum and corpus callosum; some profiles were also detected contralaterally to the traumatized hemisphere. Small numbers of reactive profiles were also identified within the ipsilateral internal capsule.

At 1, 3 and 7 days after TBI, small numbers of cortical and thalamic neuronal cell bodies were flooded with beta-APP (Fig. 1g, h). Within the cerebral cortex, abnormal neuronal staining occurred most frequently within deeper cortical layers.

Within the ipsilateral thalamus, numerous reactive profiles were observed in lateral thalamic nuclei 24 h after TBI (Fig. 2a, b). At subsequent survival periods, beta-APP axonal profiles were again seen within the vulnerable brain regions. Starting 7 days after TBI, beta-APP reactive profiles within the thalamus appeared to increase in number as compared with earlier study periods. At 30 days after TBI, focal thalamic regions including the lateral posterior and posterior thalamic nuclei displayed clusters of reactive profiles (Fig. 2c–f). Serial sections stained with hemotoxylin and eosin identified a focal region of reactive gliosis and microglial accumulation (Fig. 2f). Twenty-four h after TBI, large numbers of reactive axonal profiles were also seen within the subthalamic radiation (Fig. 2g, h).

Quantitative Findings

Quantitative assessment of beta-APP profiles within the dorsolateral striatum revealed an early increase in the number of profiles followed by a dramatic decline over time (Fig. 3a). One-way ANOVA indicated a significant effect of group ($F [3, 20] = 16.663$, $p < 0.0001$); post-hoc comparisons showed that there was a higher frequency of beta-APP reactive profiles at 24 h compared with the other survival periods.

In contrast with the striatal data, numbers of beta-APP profiles within the thalamus were initially low, but increased significantly by post-traumatic day 7 (Fig. 3b). There was an overall group effect ($F [3, 20] = 7.494$, $p < 0.002$) with post-hoc comparisons indicating that there were fewer beta-APP profiles at early periods (24 and 72 h) compared with later time points (7 and 30 days).

Similar to the dorsolateral striatal data, the internal capsule also showed an initial rise in beta-APP profiles and decline over time (Fig. 4b). One-way ANOVA on these data demonstrated an effect of group ($F [3, 20] = 3.065$, $p < 0.05$); post-hoc mean comparisons further indicated more beta-APP at 24 h vs other time periods.

An assessment of the subthalamic radiation showed an initial rise in the frequency of reactive profiles at 24 h, with a later decline in the number of profiles at subsequent study periods (Fig. 4a). An overall group effect ($F [3, 20] = 4.202$, $p < 0.02$) was found with post-hoc comparisons significant for TBI 24 h vs TBI 72 h and TBI 30 day.

Repeated measures ANOVA of the data from the external capsule also indicated significant effects of group ($F [3, 20] = 9.047$, $p < 0.0006$) and coronal level ($F [2, 40] = 37.980$, $p < 0.0001$) (Fig. 4c). Post-hoc comparisons revealed an initial increase in reactive profiles at 24 h, with a slow decline in numbers by 30 days post-TBI. An examination of numbers of beta-APP profiles by coronal level showed that the presence of beta-APP was low in sections anterior to the injury epicenter (i.e. −0.8 mm bregma), with an increasing accumulation posterior to this level (i.e. −3.8 and −6.3 mm bregma). Within the lateral somatosensory cortex, the number of beta-APP profiles did not differ significantly across survival intervals.

Comparisons between moderate and severely injured animals at 72 h post-TBI showed an increased concentration of beta-APP profiles within the severe injury group (Figs. 3, 4). One-way ANOVA indicated significant effects of group in the dorsolateral striatum, ($F [1,$

←

axonal swellings in external capsule (×1,120). (G) Reactive axonal profiles within deeper cortical layers. Several neuronal cell bodies display increased immunostaining (×280). (H) Higher magnification of cortical neuronal perikarya flooded with beta-APP immunoreactivity (×1,120).

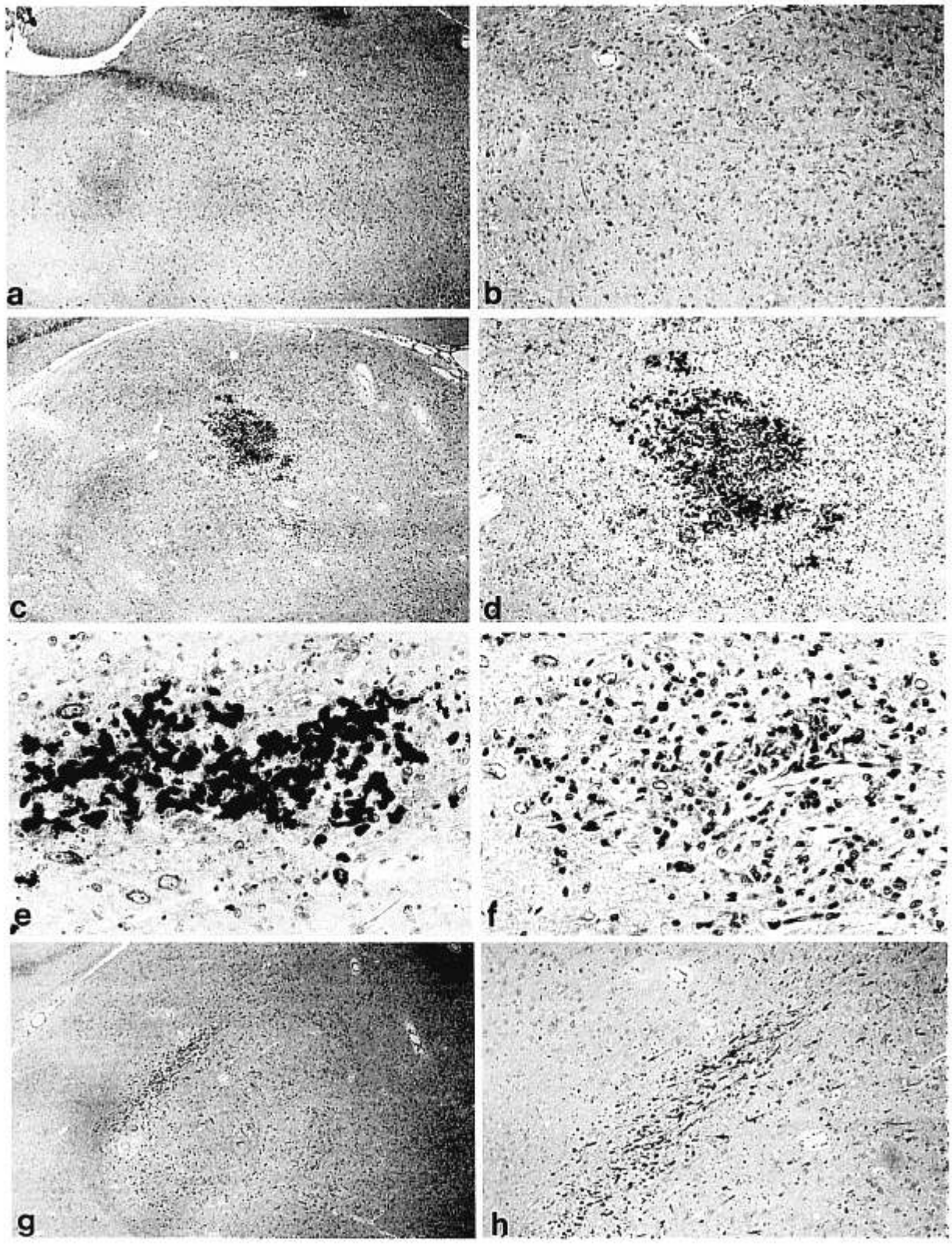

Fig. 2. Beta-amyloid precusor protein (beta-APP) –immunoreactive axons after moderate TBI. (A) At 24 h after TBI, scattered immunoreactive profiles are present within lateral thalamus (×110). (B) Higher magnification of reactive thalamic profiles (×280). (C) At 30 days after TBI, a dense cluster of reactive profiles within the thalamus (×110). (D) Higher magnification of thalamic profiles (×280). (E) Dense cluster of immunoreactive profiles within posterior thalamus 30 days after TBI (×1,120). (F) Hematoxylin and eosin–stained serial section showing that reactive profiles illustrated in Figure 2e correspond to an area of focal necrosis with reactive astrocytic and microglial accumulation (×1120). (G) At 24 h after TBI, a cluster of reactive axonal profiles within the subthalamic radiation (×110). (H) Higher magnification showing individual axonal profiles within radiation (×280).

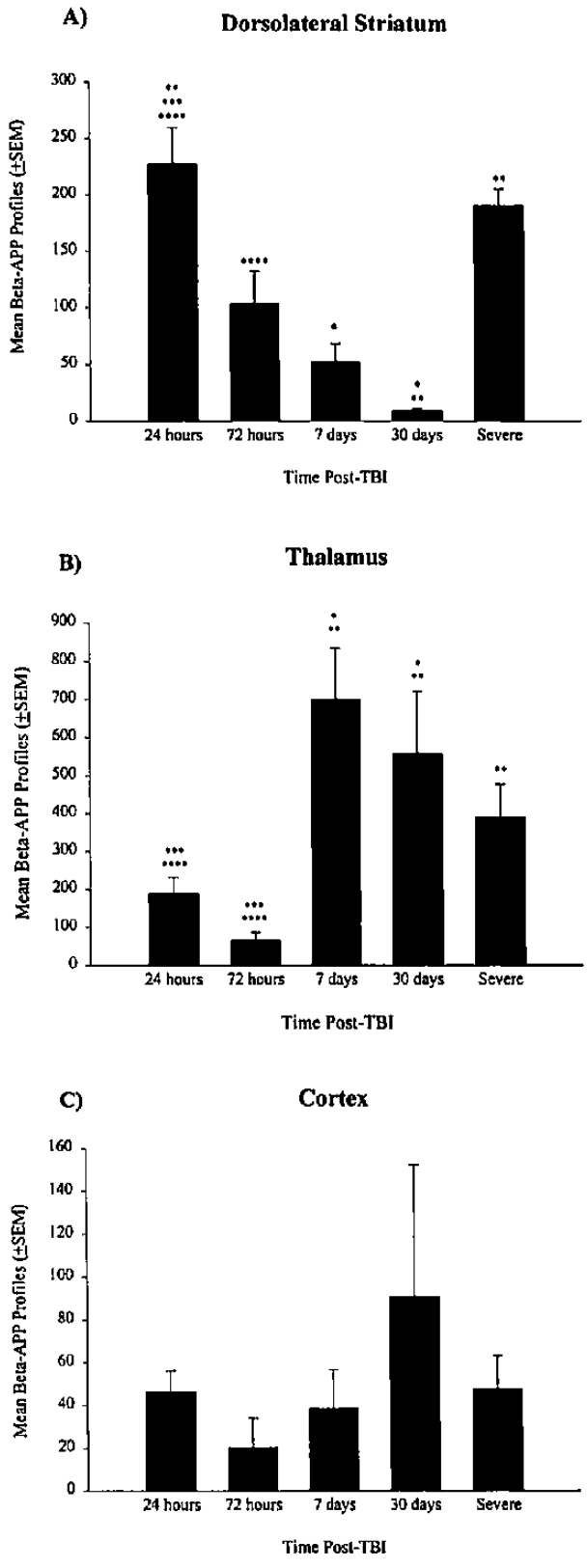

Fig. 3. Bar graphs of mean ± SEM of numbers of beta-APP–positive axonal profiles per microscopic field within gray matter structures. (A) Early increase in beta-APP profiles in dorsolateral striatum followed by a decline at later time periods. At 72 h after TBI, severely injured rats demonstrate significantly more reactive profiles compared with moderately injured rats. (B) A late increase in the frequency of beta-APP profiles is observed within the thalamus. Severely injured rats displayed increased numbers of reactive profiles compared with moderate injury. (C) Reactive profiles within cerebral cortex. (*$p < 0.05$ vs TBI-24; ** $p < 0.05$ vs TBI-72; *** $p < 0.05$ vs TBI-7; **** $p < 0.05$ vs TBI-30).

10] = 7.260, $p < 0.03$), thalamus (F [1, 10] = 12.704, $p < 0.006$), and subthalamic radiation (F [1, 10] = 23.153, $p < 0.0004$). Repeated measures analysis for the external capsule showed significant effects of both group (F [1, 10] = 5.213, $p < 0.05$) and coronal level (F [2, 20] = 22.846, $p < 0.0001$). Thus, there was an increase in the number of beta-APP profiles at each coronal level analyzed for the severe vs moderately injured animals.

DISCUSSION

The temporal course and pathobiology of axonal damage after human and experimental brain injury has been discussed in various comprehensive publications (28–31). In human head injury, evidence for axonal damage has been reported as early as 2 h after injury using beta-APP as a marker of axonal damage (13). Blumbergs and colleagues have developed a sector scoring method using beta-APP to determine the extent of DAI after mild or severe head trauma (32). In an ultrastructural study, Maxwell and colleagues (33) reported evidence for axon shearing as early as 25-35 min after lateral acceleration injury in nonhuman primates. Using the immunocytochemical visualization of neurofilament subunits as an indicator of axonal damage, Yaghmai and Povlishock (8) reported intensely 68 kD-immunoreactive axonal segments within one h after controlled cortical impact and F-P injury. The most conspicuous anatomical sites for these axonal changes included the ponto-medullary junction, cerebellar peduncles, the vestibular and red nuclei, the cranial nerves coursing through the brain stem, the internal and external capsules, as well as the corpus callosum. Pierce and colleagues (16) reported APP/APLP accumulation in axonal swellings beginning 2 h and persisting up to 2 weeks after F-P brain injury. Thus, clinical and experimental data demonstrate that TBI can produce early membrane perturbations and an impairment in axoplasmic transport, leading to continued axonal swelling and axonal detachment (31, 34–36).

Recently, a new model of TBI without focal brain lesions has been developed in rats to induce widespread axonal injury (37). With this intact skull weight-drop model, Foda and Marmarou (38) reported DAI that primarily involved the corpus callosum, internal capsule, optic tracts, cerebral peduncles and the long tracts of the brainstem. In the present study, axonal damage within

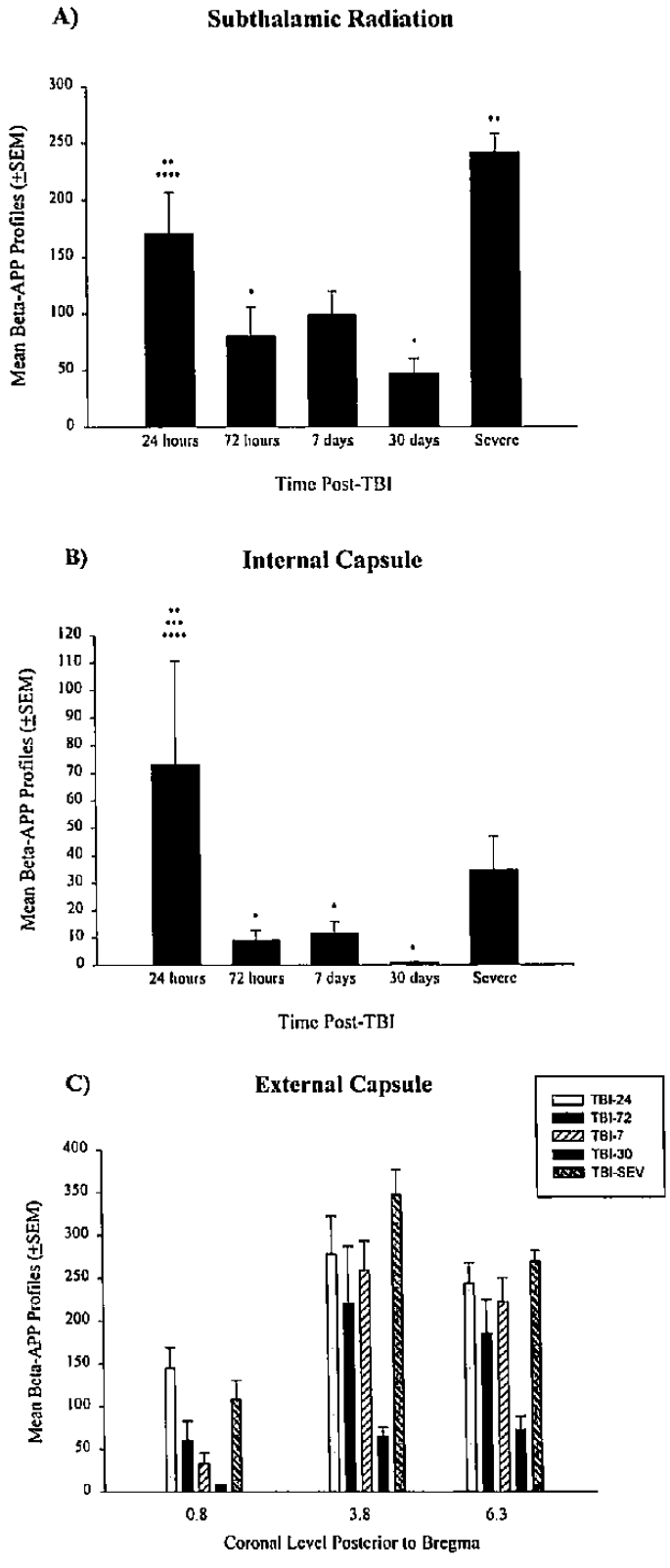

Fig. 4. Bar graphs of mean ± SEM of numbers of beta-APP–positive axonal profiles per microscopic field within white matter tracts. (A) Early increase in reactive axonal profiles within the subthalamic radiation with reduced numbers at subsequent time periods. Severely injured rats displayed a higher frequency of reactive profiles as compared with moderate injury. (B) A transient increase in reactive profiles within the internal capsule. (C) A transient increase in reactive profiles within the external capsule at coronal levels anterior to injury epicenter (0.8 mm bregma). However, a sustained increase in reactive profiles was observed within the external capsule at more posterior levels (−3.8 and −6.3 mm bregma).(* $p < 0.05$ vs TBI-24; ** $p < 0.05$ vs TBI-72; *** $p < 0.05$ vs TBI-7; **** $p < 0.05$ vs TBI-30).

forebrain regions may have resulted in part from shear forces generated by the parasagittally positioned impact site. Previous morphological studies have documented mechanically disrupted pial and parenchymal vessels after moderate TBI (17, 39) and similar strains generated by the primary impact might have participated in the present axonal changes. Such a mechanism might be most active within the external capsule where evidence for mechanical damage to blood vessels is reported (17).

Data consistent with reversible axonal damage was obtained within the dorsolateral striatum and the anterior external capsule after moderate TBI. Within these structures, an initial increase at day 1 in the frequency of reactive axonal profiles was followed by a decrease at subsequent time periods. In contrast, an early but sustained increase in reactive profiles occurred within the external capsule at coronal levels corresponding to the injury epicenter. Reversible abnormalities in axonal transport after moderate TBI are potentially important in the understanding of mechanisms underlying transient dysfunction after TBI. In addition, it is possible that secondary injury mechanisms (40–42) might aggravate traumatic outcome by converting these reversible changes into irreversible consequences.

However, it is not fully known whether the transient effects seen in the striatum are truly reversible. The damage reflected by the staining may be caused by an injury at the origin of the cell body for these axons. Therefore, the changes observed may be transient due to the rapid loss of the entire process. Another possibility is that injury to collateral projections from the corticospinal and corticobulbar tracts is producing this effect. An injury to these collaterals may produce a different profile than one that involves the main axonal shaft. Future studies to clarify the reversibility of the damage could use silver staining as a marker for Wallerian changes or electron microscopy studies using beta-APP to describe what is occurring at the ultrastructural level.

The importance of injury severity on the degree of axonal damage after TBI was also demonstrated in this study. At 3 days after trauma, severe TBI resulted in significantly greater numbers of reactive axonal profiles in the striatum, thalamus, and internal capsule compared with moderate injury. In reference to injury severity, Perri and colleagues (43) reported that injury severity is an

important factor in determining lesion volume after F-P injury. In addition, autoradiographic cerebral blood flow studies have demonstrated more severe hemodynamic reductions following severe versus moderate F-P injury (43). Based on current concepts indicating that TBI does not necessarily trigger immediate or irreversible damage to axons (30), injury severity appears to be an important factor in determining the temporal response and reversibility of axonal abnormalities after TBI.

Although DAI plays a major role in the morbidity and mortality associated with head injury, few therapeutic strategies to date have been advanced that target this important outcome measure. Posttraumatic hypothermia has been shown in experimental (18, 20, 27, 44–46) and clinical studies (47,48) to provide protection in terms of morphological and functional outcome. In regards to the present discussion, posttraumatic hypothermia (33 to 34°C) and the 21-aminosteroid, U-74389G have been reported to reduce the number of damaged axons in the internal capsule after controlled cortical contusion (49). In contrast, delayed posttraumatic hyperthermia (39°C) significantly aggravates the axonal consequences of F-P injury (19). Based on the present data, it would appear that therapeutic strategies directed against DAI could be regionally selective, with the beneficial effects being dependent on injury severity.

Thalamic damage after brain injury has been reported in clinical and experimental studies (20, 23, 24, 50). In human brain injury, Ross and colleagues (50) documented the selective loss of neurons within the reticular nucleus in patients with severe head injuries. In a study by Anderson et al, (24), patients with moderate to severe injuries had reduced thalamic volumes. In the present study, the most severe thalamic changes appeared relatively late after F-P brain injury. Because thalamic neurons have reciprocal connections with the parietal cortex (51), these structural changes may be related to connectivity and direct damage to cortical neurons (15). From a therapeutic standpoint, the delay in thalamic abnormalities might indicate an extended window for posttraumatic treatment. In this regard, treatment with the neurotrophic factor basic fibroblast growth factor (bFGF) has been reported to protect against thalamic atrophy after middle cerebral artery occlusion (52) and to decrease contusion volume and cognitive dysfunction after F-P injury (53, 54). It would therefore be important in future studies to determine whether treatment with potentially neuroprotective agents including bFGF would attenuate the thalamic damage reported in this study.

The abnormal accumulation of beta-APP was also detected within the perikaryon of cortical and thalamic neurons after TBI. Cortical neurons overlying the contusion site were flooded with beta-APP at 1 and 3 days after injury. This response was quite different from the staining characteristics seen in sham-operated controls. Pierce and colleagues (16) also reported increased APP/APLP immunoreactivity in a small number of neuronal perikaryon within the thalamus and cortex 2 and 7 days after F-P brain injury. Although the significance of beta-APP accumulation within neuronal cell bodies is not known, it may be a response of the continued synthesis of beta-APP and the inhibition of normal axoplasmic transport due to axonal damage. Shigematsu and McGeer (55) reported that the administration of agents that selectively disrupt axoplasmic transport leads to the abnormal accumulation of APP in cell bodies. Alternatively, TBI-induced neuronal injury may lead to an increased synthesis of beta-APP and abnormal accumulation.

Although the function of beta-APP is not well understood (56–58), beta-APP under certain circumstances gives rise to beta amyloid, a protein that is found in senile plaques of Alzheimer disease (59). Recently, the physiologically secreted form of beta-APP has been documented to protect cultured neurons against excitotoxic or hypoglycemic insults by reducing intracelluar Ca^{2+} and modifying calcium responses to glutamate (60). In addition, Smith-Swintosky et al (61) reported that the postischemic administration of the secreted form of beta-APP protected CA1 pyramidal neurons from a transient ischemic insult. In contrast, aggregated forms of beta-amyloid peptide have been reported to be neurotoxic (62, 63). The ultimate outcome of beta-APP flooded neurons in terms of long-term survival after TBI remains to be determined.

In summary, the present study provides new information regarding the temporal and regional patterns of widespread axonal damage after F-P brain injury. These data may demonstrate reversible and irreversible axonal perturbations occurring within specific brain regions with moderate injury levels. Within the thalamus, a more delayed axonal response was reported. Widespread axonal damage in combination with selective patterns of neuronal necrosis most likely contributes to ventricular dilation after chronic F-P injury (20). Finally, increased injury severity led to a more severe axonal response. These findings provide baseline data for future studies directed at understanding the functional importance of widespread axonal changes after TBI and for the assessment of treatment strategies directed against axonal pathology.

REFERENCES

1. Adams JH, Doyle D, Ford I, Genarelli TA, Graham DI, McLellan DR. Diffuse axonal injury in head injury. Definition, diagnosis and grading. Histopathology 1989;15:49–59
2. McLellan DR, Adams JH, Graham DI. The structural basis of the vegetative state and prolonged coma after non-missile head injury. In: Papo I, Cohadon F, Massarotti M, eds. Le Coma Traumatique. Padova: Liviana Editride, 1986:165–72

3. Graham DI. Neuropathology of head injury. In: Narayan RK, Wilberger JE, Povlishock JT, eds. Neurotrauma. New York: McGraw-Hill, 1996:43–59
4. Adams JH. Head injury. In: Adams JH, Cuchen LW, eds. Greenfield's Neuropathology. Oxford University Press, New York, 1992: 106–52
5. Vanezis P, Chan KK, Scholtz CL. White matter damage following acute head injury. Forensic Sci Int 1987;35:1–10
6. Grady MS, McLaughlin MR, Christman CW, Valadk AB, Kligner CL, Povlishock JT. The use of antibodies targeted against the neurofilament subunits for the detection of diffuse axonal injury in humans. J Neuropathol Exp Neurol 1993;42:143–52
7. Christman CW, Grady MS, Walker SA, Holloway KL, Povlishock JT. Ultrastructural studies of diffuse axonal injury in humans. J Neurotrauma 1994;11:173–86
8. Yaghmai A, Povlishock JT. Traumatically induced reactive changes as visualized through the use of monoclonal antibodies targeted to neurofilament subunits. J Neuropathol Exp Neurol 1992:158–76
9. Blumbergs PC, Scott G, Manavis J, Wainwright H, Simpson DA, McLean AJ. Staining of amyloid precursor protein to study axonal damage in mild head injury. Lancet 1994;344:1055–56
10. Roberts GW, Gentleman SM, Lynch A, Graham DI. BetaA4 amyloid protein deposition in brain after head trauma. Lancet 1991; 338:1422–23
11. Gentleman SM, Nash MJ, Sweeting CJ, Graham DI, Roberts GW. Beta-amyloid precursor protein (beta APP) as a marker for axonal injury after head injury. Neurosci Lett 1993;160:139–44
12. Sheriff FE, Bridges LR, Sivaloganthan S. Early detection of axonal injury after human head trauma using immunocytochemistry for beta-amyloid precursor protein. Acta Neuropathol 1994:55–62
13. McKenzie KJ, McLellan DR, Gentleman SM, Maxwell WL, Gennarelli TA, Graham DI. Is beta-APP a marker of axonal damage in short-surviving head injury? Acta Neuropathol 1996;92:608–13
14. Ostsuka N, Tomonaga M, Ikeda K. Rapid appearance of beta-amyloid percusor protein immunoreactivity in damaged axons and reactive glial cells in rat brain following needle stab injury. Brain Res 1991;568:335–38
15. Lewen A, Li GL, Nilsson P, Olsson Y, Hillered L. Traumatic brain injury in rat produces changes of beta-amyloid precursor protein immunoreactivity. NeuroReport 1995;6:357–60
16. Pierce JES, Trojanowski JQ, Graham DI, Smith DH, McIntosh TK. Immunohistochemical characterization of alterations in the distribution of amyloid precursor proteins and beta-amyloid peptide after experimental brain injury in the rat. J Neurosci 1996;16:1083–90
17. Dietrich WD, Alonso O, Halley M. Early microvascular and neuronal consequences of traumatic brain injury in rats. A light and electron microscopic study. J Neurotrauma 1994a;11:289–301
18. Dietrich WD, Alonso O, Busto R, Globus MY-T, Ginsberg MD. Post-traumatic brain hypothermia reduces histopathological damage following concussive brain injury in the rat. Acta Neuropathol 1994b;87:250–58
19. Dietrich WD, Alonso O, Halley M, Busto R. Delayed posttraumatic brain hyperthermia worsens outcome after fluid percussion brain injury: A light and electron microscopic study in rats. Neurosurgery 1996;38:533–41
20. Bramlett HM, Dietrich WD, Green EJ, Busto R. Chronic histopathological consequences of fluid-percussion brain injury in rats: Effects of post-traumatic hypothermia. Acta Neuropathol 1997;93: 190–99
21. MacNamara SE, Bigler ED, Blatter D. Magnetic resonance identified ventricular dilation in traumatic brain injury: Comparison of pre- and post-injury scan and postinjury results. Arch Clin Neuropsychiatr 1992;7:275–84
22. Anderson CV, Bigler ED. The role of caudate nucleus and corpus callosum atrophy in trauma-induced anterior horn dilation. Brain Inj 1994;8:565–69
23. Anderson CV, Bigler ED. Ventricular dilation, cortical atrophy, and neuropsychological outcome following traumatic brain injury. J Neuropsychiatry 1995;7:42–48
24. Anderson CV, Wood D-MG, Bigler ED, Blatter DD. Lesion volume, injury severity, and thalamic integrity following head injury. J Neurotrauma 1996;13:35–40
25. Paxinos G, Watson C. The rat brain in stereotaxic coordinates. Academic Press, New York, 1982
26. Dixon CE, Lyeth BG, Povlishock JT, et al. A fluid percussion model of experimental brain injury in the rat. 1987;67:110–19
27. Clifton GL, Jiang, JY, Lyeth BG, Jenkins LW, Hamm RJ, Hayes RL. Marked protection by moderate hypothermia after experimental traumatic brain injury. J Cereb Blood Flow Metab 1991;11:114–21
28. Povlishock JT. Pathobiology of traumatically induced axonal injury in animals and man. Ann Emerg Med 1993;22:41–47
29. Gennarelli TA, Thibault LE, Adams JH, Graham DI, Thompson CJ, Marcincin RP. Diffuse axonal injury and traumatic coma in the primate. Ann Neurol 1982;12:564–74
30. Povlishock JT, Jenkins LW. Are the pathobiological changes evoked by traumatic brain injury immediate and irreversible? Brain Pathol 1995;5:415–26
31. Povlishock JT. Traumatically induced axonal injury: Pathogenesis and pathobiological implications. Brain Pathol 1992;2:1–12
32. Blumbergs PC, Scott G, Manavis J, Wainwright H, Simpson DA, McLean AJ. Topography of axonal injury as defined by amyloid precursor protein and the sector scoring method in mild and severe closed head injury. J Neurotrauma 1995;12:565–72
33. Maxwell WL, Watt C, Graham DI, Gennarelli TA. Ultrastructural evidence of axonal shearing as a result of lateral acceleration of the head in non-human primates. Acta Neuropathol 1993;86:136–44
34. Pettus EH, Povlishock JT. Characterization of a distinct set of intra-axonal ultrastructural changes associated with traumatically induced alteration in axolemmal permeability. Brain Res 1996;772:1–11
35. Povlishock JT, Pettus EH. Traumatically induced axonal damage: Evidence for enduring changes in axolemmal permeability with associated cytoskeletal change. Acta Neurochir (Supp) 1996;66:81–86
36. Pettus EH, Christman CW, Giebel ML, Povlishock JT. Traumatically induced altered membrane permeability: Its relationship to traumatically induced reactive axonal change. J Neurotrauma 1994; 11:507–22
37. Marmarou P, Foda MA, van den Brink WV, Kita H, Demtriadou K. A new model of diffuse brain injury in rats. Part I: Pathophysiology and biomechanics. J Neurosurg 1994;80:291–300
38. Foda MA, Marmarou A. A new model of diffuse brain injury in rats. Part II: Morphological characterization. J Neurosurg 1994;80: 301–13
39. Maxwell WL, Whitfield PC, Suzen B, Graham DI, Adams JH, Watt C, Gennarelli TA. The cerebrovascular response to experimental lateral head acceleration. Acta Neuropathol 1992;84:289–96
40. Jenkins LW, Moszynski K, Lyeth BG, et al. Increased vulnerability of the mildly traumatized rat brain to cerebral ischemia: The use of controlled secondary ischemia as a research tool to identify common or different mechanisms contributing to mechanical and ischemic brain injury. Brain Res 1089;477:211–24
41. Chesnut RM. Secondary brain insults after head injury: Clinical perspectives. New Horizons 1995;3:366–75
42. Dietrich WD, Alonso OF, Busto R, Loor J, Dewanjee MK, Ginsberg MD. Cerebral ischemia following traumatic brain injury in rats [abstract]. J Cereb Blood Flow Metabol 1997;17 (Suppl 1):S83
43. Perri BR, Smith DH, Mural H, Sinson G, Saatman KE, Raghupathi R, Bartus RT, McIntosh TK. Metabolic quantification of lesion volume following experimental traumatic brain injury in the rat. J Neurotrauma 1997;14:15–22

44. Jiang JY, Lyeth BG, Kapasi MZ, Jenkins LW, Povlishock JT. Moderate hypothermia reduces blood-brain barrier disruption following traumatic brain injury in the rat. Acta Neuropathol 1992;84:495–500
45. Lyeth BG, Jiang JY, Liu S. Behavioral protection by moderate hypothermia initiated after experimental traumatic brain injury. J Neurotrauma 1993;10:57–64
46. Bramlett HM, Green EJ, Dietrich WD, Busto R, Globus MY-T, Ginsberg MD. Posttraumatic brain hypothermia provides protection from sensormotor and cognitive behavioral deficits. J Neurotrauma 1995;12:289–98
47. Clifton GL, Allen S, Barrodale P, Plenger P, Berry J, Koch S, Fletcher J, Hayes RL, Choi SC. A phase II study of moderate hypothermia in severe brain injury. J Neurotrauma 1993;10:263–71
48. Marion DW, Penrod LE, Kelsey SF, Obrist WD, Kochanek PM, Palmer AM, Wisniewski SR, DeKosky ST. Treatment of traumatic brain injury with moderate hypothermia. New Eng J Med 1997; 336:540–46
49. Marion DW, White MJ. Treatment of experimental brain injury with moderate hypothermia and 21-aminosteroids. J Neurotrauma 1996; 13:139–47
50. Ross DT, Graham DI, Adams JH. Selective loss of neurons from the thalamic reticular nucleus following severe head injury. J Neurotrauma 1993;10:151–65
51. Price JL. Thalamus. In: The rat nervous system. Paxinos G, ed. Academic Press 1995:629–48
52. Yamada K, Kinoshita A, Kohmura E Sakaguchi T, Taguchi J, Kataoka K, Hayakawa T. Basic fibroblast growth factor prevents thalamic degeneration after cortical infarction. J Cereb Blood Flow Metab 1991;11:472–78
53. Dietrich WD, Alonso O, Busto R, Finklestein SP. Posttreatment with intravenous basic fibroblast growth factor reduces histopathological damage following fluid-percussion brain injury. J Neurotrauma 1996;13:309–16
54. McDermott KL, Raghupathi R, Fernandez SC, et al. Delayed administration of basic fibroblast growth factor (bFGF) attenuates cognitive dysfunction following parasagittal fluid percussion brain injury in the rat. J Neurotrauma 1997;14:191–200
55. Shigematsu K, McGeer PL. Accumulation of amyloid precusor protein in neurons after intraventricular injection of colchicine. Am J Pathol 1992;140:787–94
56. LeBlanc AC, Kovacs DM, Chen HY, Villare F, Tyocinski M, Autilio-Gambetti L, Gambetti P. Role of amyloid precursor protein (APP); Study with antisense transfection of human neuroblastoma cells. J Neurosci Res 1992;31:635–45
57. Shigemtsu K, McGreer PL, Walker DG, Ishii T, McGeer EG. Reactive microglia/macrophages phagocytose amyloid precursor protein produced by neurons following neural damage. J Neurosci Res 1992;31:443–53
58. Schubert D, Jin L-W, Saitoh T, Cole G. The regulation of amyloid beta protein precursor secretion and its modulatory role in cell adhesion. Neuron 1989;3:689–94
59. Shoji M, Golde TE, Cheung J, et al. Production of the Alzheimer amyloid beta protein by normal proteolytic processing. Science 1992;258:126–29
60. Mattson MP, Cheng B, Culwell AR, Esch FS, Lieberburg I, Rydel RE. Evidence for excitoprotective and intraneuronal calcium-regulating roles of secreted forms of beta-amyloid precusor protein. Neuron 1993;10:243–54
61. Smith-Swintosky, VL, Pettigrew LC, Craddock SD, Culwell AR, Rydel RE, Mattson MP. Secreted forms of beta-amyloid precursor protein protect against ischemic brain injury. J Neurochem 1994; 63:781–84
62. Koh JY, Yang LL, Cotman CW. Beta-amyliod protein increases the vulnerability of cultured cortical neurons to excititoxic damage. Brain Res 1990;533:315–20
63. Pike CJ, Walencewicz AJ, Glabe CG, Cotman CW. In vitro aging of beta-amyloid protein causes peptide aggregation and neurotoxicity. Brain Res 1991;563:311–14

Received June 4, 1997
Accepted July 30, 1997